

Investigation of local cathodic protection of carbon steel pipe by immersed current method

Sahar K.Abod*, Basim O.Hasan

Department of Chemical Engineering, Al-Nahrain, University, Iraq

*Corresponding author Email: Sahar.mche23@ced.nahrainuniv.edu.iq

(Received 22 Aug, Revised 3 Oct, Accepted 5 Oct)

Abstract: The cathodic protection (CP) is widely used in the oil and gas industry to prevent (or reduce) corrosion of structures and metal pipelines. To guarantee a more effective CP system, an applicable design for the under-protected structures is required. The potential decay on steel structure surface, due to being away from the power source, can cause a considerable local protection deficiency of parts of the structure due to the enhanced corrosion attack. In the present work, the local cathodic protection of carbon steel pipe in different concentrations (0.01 N, 0.05 N, 0.1N) of NaCl solution were investigated and discussed. Quantitative values of the effect of potential decay on the protection efficiency and on the immersed current were reported under different operating conditions such as anode to cathode area ratio, anode to cathode distance. The use high ratio of graphite to CS structure at 1.2, gave high protection percentage (at a concentration 0.01 N and h= 100 mm) reaching up to 96% for CS1 while the CS2 showed a lower protection rate of about 88%, and the CS3 that was farther from the energy source had a lower protection rate of 82%, as it was noted that the corrosion rate is increase with increasing salt concentration and decrease with increasing area ratio

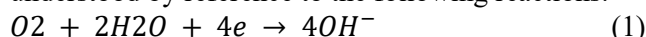
Keywords: cathodic protection, local position, immersed current, carbon steel, salt solution.

1. Introduction

One of the biggest challenges facing our aging infrastructures is material loss and deterioration by electrochemical reactions that cause corrosion [1-3]. A study by the Federal Highway Administration of the United States showed that the total direct cost of corrosion in the United States alone was \$279 billion per year, which is about 3.2 percent of the nation's present gross domestic product (GDP). Corrosion compromise's structure safety and is a leading factor in the catastrophic failure of bridges, nuclear facilities, airplane components, and equipment used in chemical, petrochemical, transportation, and construction industries. Corrosion is a spontaneous, slow-progressing phenomenon [2,4]. Corrosion is an electrochemical process involving the passage of electrical currents on a micro or macro scale. The change from the metallic to the combined form occurs through an anodic reaction:



The mechanism of cathodic protection is simply understood by reference to the following reactions.



Various methods of preventing corrosion in the aquatic area had been developed. One of them is cathodic protection using a sacrificial anode and impressed current method [5]. Cathodic protection is a more reliable, effective, and economical method for the protection of a variety of pipelines, tanks, marine structures including ships hulls, and submarines against corrosion. Cathodic protection works primarily by depressing the natural corrosion potential of the structure to be protected to a value where it does not corrode. Cathodic protection systems are most commonly used to protect steel, water/fuel pipelines and storage tanks; steel pier piles, ships, offshore oil platforms, and onshore oil well casings among others [6].

DOI: <https://doi.org/10.61263/mjes.v3i2.101>

This work is licensed under a [Creative Commons Attribution 4.0 International License](https://creativecommons.org/licenses/by/4.0/).



Impressed-current systems employ inert anodes and use an external source of DC power to impress a current from an external anode onto the cathode surface, the impressed current cathodic protection is used for larger structures that galvanic anodes could not economically deliver current to provide complete protection[7]. Metal that has been extracted from its primary ore (metal oxides or other free radicals) naturally tends to revert to that state under the action of oxygen and water. This phenomenon is known as corrosion, with rusting of steel being the most common example. In seawater, the increase of the interfacial pH due to CP induces the formation of a mineral layer on the steel surface. The increase of pH at the steel/seawater interface is due to the increase of the cathodic reaction rate, a direct consequence of the cathodic polarization. In most cases, the main reaction involved is the reduction of dissolved O₂[8].

Making the surface more negative and increasing the concentration of electrons accelerates the rate of the cathodic reaction and decreases the rate of the anodic reaction. (i.e. the rate of the anodic reaction becomes zero and the whole surface of the metal becomes cathodic. Anodes in impressed current systems are usually made of graphite, high silicon iron, and scrap iron. The system connects the anode to the structure via an insulated wire through which current flows from the anode through the electrolyte onto the structure. Graphite has the advantages of long-life corrosion protection, low maintenance cost, and high efficiency. These are generally cylindrical, and although other forms are available, it has the advantage of being cheap and abundantly available [9,10].

Extensive literature depicts numerous studies that have been conducted concerning the utilization of immersed current for cathodic protection in diverse environmental settings, yielding a range of outcomes. Ajeel et al., [2007] This system was used to investigate the influence of various conditions on the minimum cathodic protection current that would provide full cathodic protection for steel tubes

immersed in sea water. The variable conditions studied are the concentration of (0.01 – 3.5) % NaCl, temperature (30- 50°C), the distance between pipe (cathode) and graphite electrode (anode) of (10 – 20) cm, and pH solution of (5.0 – 9.0) using a selected range of these conditions, the experimental results for the minimum cathodic protection current were obtained and recorded. The electrochemical results show that cathodic protection current density increases with increasing temperature and concentration. The current density also slightly increases with increased distance between the cathode and anode. Redaelli et al., [2014] A combined experimental and numerical investigation was carried out to determine whether a few localized galvanic anodes per unit length could protect the reinforcement of slender carbonated concrete elements, exposed to atmospheric conditions, Results showed that, despite the high electrical resistivity of carbonated concrete, anodes with a spacing of 0.45 m are enough to protect corroding reinforcement in most exposure conditions, even in thin parts of the element. Matloub et al., [2018] The study examined the corrosion rate of pipelines in water with different salt concentrations. Cathodic protection, along with various coatings, was found to be the best method of protection. The experiments involved different cathodic currents, pH values, and NaCl concentrations. Full cathodic protection resulted in a low corrosion rate of 0.3445 mm/year. However, the corrosion rate increased with decreasing pH and increasing salt concentration. Bhuiyan et al., [2019] In this study, the effectiveness of impressed current cathodic protection (ICCP) in preventing corrosion of steel reinforcement in concrete was investigated. The study examined how the distance of the anode from the steel and the level of corrosion affect the distribution of current. The researchers applied a potential sweep and measured the steel potential and current for specimens with three layers of steel at different depths. The findings showed that there is an inverse relationship between cathodic polarization and the distance of the steel from the anode. Additionally, higher levels of corrosion can lead to a more non-uniform current distribution, favoring the closest bar to the anode. Avianto et al., [2020] When carbon steel pipes touch, they can corrode faster, so we ran simulations to determine the best distance between anodes to protect the 20-inch pipe installation project. We found that only at a 15-meter distance could we achieve the minimum required protection. Installing anodes at 15-meter intervals with pairs of anodes spaced 4.9 meters apart met the minimum potential for corrosion protection according to the simulation results. BAWA et al., [2020] Investigated locally made anodes of different materials in harsh soil saturated with sodium chloride solution. Corrosion cells were created by burying pipelines with four anodes. I monitored their performance, depletion period, and electrochemical behavior. The lead-based anode displayed good protection, with only 10.22% depletion

after twenty-one days of testing. Li & Du, [2022] Chloride ions in marine environments can cause corrosion in structural steel. A study examined the impact of chloride ion content on pitting corrosion of Dispersion-Strengthened-High-Strength steel. High chloride ion content reduced dissolved oxygen, slowing corrosion. In high chloride ion solutions, the formation of α -FeOOH was inhibited, weakening corrosion product protection.

Guma et al., [2016] In the study, corrosion protection (CP) using pure magnesium and magnesium alloy as galvanic anodes was found to be effective in preventing corrosion in structures. The research showed that corrosion rates could be significantly reduced by polarizing structures to -0.85V versus Cu/CuSO₄ electrodes with the anodes. Pure magnesium was the most cost-effective and efficient anode for CP, followed by magnesium alloy. Each unit surface area of the anodes can protect nearly 1200 units of the structure at the -0.85V protective potential, depending on the type of anode.

Through previous studies in this field, it has been observed that there is limited research on the topics of local cathodic protection and potential decay. These areas require further investigation under different real-world conditions. In practice, cathodic protection is subjected to varying circumstances, where it may be stronger in some areas and weaker in others, leading to local deficiencies. Therefore, more studies are needed to address these gaps.

Therefore, this work aims to assess the impact of potential decay on the local cathodic protection of carbon steel pipes in different salt solutions, using the graphite-immersed current cathodic protection method. Additionally, this study will examine the effect of the distance between the anode and cathode and the anode-to-cathode area ratio on local cathodic protection.

2. Experimental work

Figure 1 shows the experimental setup which comprises a basin of dimensions 900×450×400 mm containing the corrosive solution, a voltmeter to measure the structure potential, an ammeter to measure the current, DC Adjustable power supply, type DAZHENG, Model APS-3005D, Voltage Output 0-30V, Current Output 0-5A, a standard calomel electrode (SCE) as a reference electrode, and a heater and controller to set the required temperature. Digital balance of high accuracy (4 decimal places of a gram) to measure the weight loss. Optical Microscope (type of KRUS/ Germany) was used for surface inspection after corrosion and after applying cathodic protection. Pure graphite (cylinder) of various dimensions was used as anode. Three different NaCl solutions were used (0.01N, 0.05N, 0.1N) at 30 °C. The local cathodic protection of carbon steel pipe was quantified by determining the cathodic protection percent for three specimens of different local positions from the anode (the graphite). These specimens were connected by a highly conductive wire to behave as different local positions on one pipe. Therefore, each specimen represents specific location on the pipe. Each carbon steel specimen used was a cylindrical rod with dimensions of 100 mm long and 10 mm in diameter. The graphite specimen sheet dimensions were used as a sacrificial anode with dimensions of (40×80×240 mm). Three values of anode-to-cathode distance were investigated namely, 100, 200, 400 mm, and Acs) different values of anode-to-cathode area ratios (AR). The anode-to-cathode area ratios (A_{gr}/ investigated were 5% and 10%, and the anode-to-cathode distance (D) were 100 mm, 200mm, and 400 mm. Three values of inter-specimens' distance (h) were investigated namely 100 mm, 200 mm, and 400 mm. The setup of the local position of each specimen relative to the anode is shown in Fig.2. The SCE was placed close to the specimens at about 1-2 mm to measure the potential versus time of both the cathode structure and the graphite anode.

The chemical composition of the pipe is presented in Appendix (Table A-1) and Fig (A-1). The analysis of the specimen composition was carried out in the Ministry of Science and Technology.

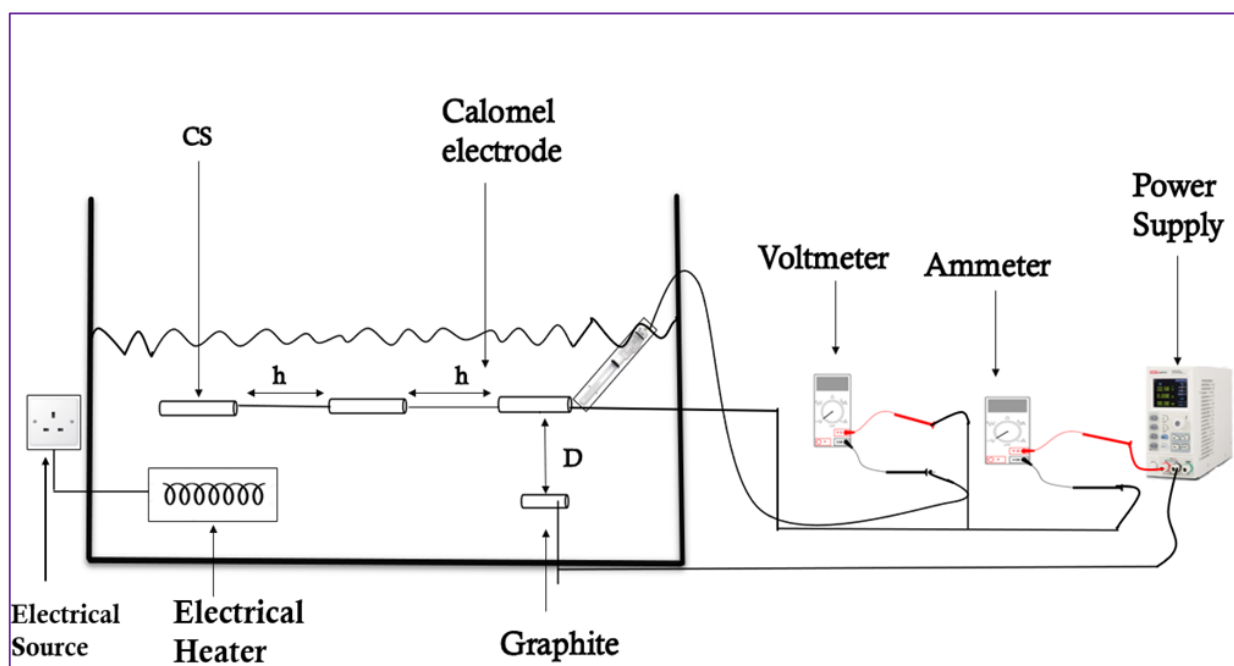


Fig. 1. Experimental setup

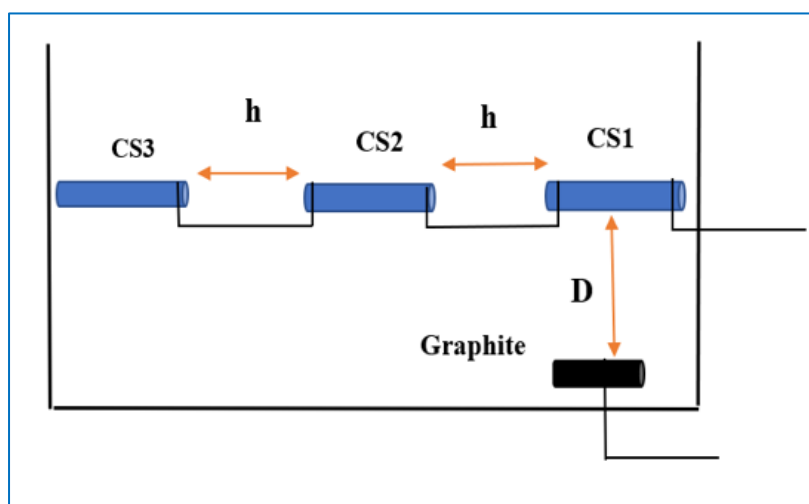


Fig. 2. Connection and distances between the specimens and the anode

The first part of the experiments included the determination of the free corrosion rate and potential of CS

before applying the CP using the weight loss method. To measure the weight loss, the specimens (CS) were carefully prepared through a series of steps. This included using emery papers at varying levels (400 and 2000) to ensure a clean and dirt-free surface. The specimen was then thoroughly washed with distilled water and dried with a clean tissue. Next, it was immersed in methanol for one minute to remove any remaining deposits. The specimen was then washed with distilled water, dried by clean tissue, and then placed in an oven at 80°C for 5 minutes. Afterward, the specimen was placed in a vacuum desiccator containing high-activity silica gel. The sample's original weight was then recorded. Next, a solution of (0.01,0.05 and 0.1N) sodium chloride The sample was placed in the solution and allowed to corrode for three hours[18-20]. Following this period, the sample was removed, washed with distilled water, and gently brushed with a plastic brush to remove any corrosion product layer. Finally, the sample was dried with a clean tissue and immersed in acetone for one minute, dried, and weighed to determine the weight loss . The corrosion rate was obtained using the following equation [21]

$$CR \text{ (in gmd)} = \frac{\text{weightloss(g)}}{\text{Area(m}^2\text{)} \times \text{Time (day)}} \quad (3)$$

Where: (gmd): gram /m².day.

When applying the cathodic protection (CP) the same procedure was followed to obtain the weight loss in the presence of CP. The NaCl solution was prepared and heated in the water to constant temperatures of 30°C. Then, the specimen was immersed in the solution and the electrical circuit was switched on. The circuit current, CS potentials, potential was recorded with time until the end of the test duration which was 3 h. When applying the cathodic protection, the protection efficiency of single specimen was determined first for different anode to cathode distance. Then, the local cathodic protection efficiency of a setup of the three specimens connected in series was determined. The three samples were placed at different distances from the connection point of the CS pipe with the anode in the corrosive solution. The distance between first sample and the anode which was graphite, was D= 200 mm. The inter-distance between the three local positions (h) was varied. To determine the protection percentage (CP), the following formula was used[10]:

$$CP\% = \left(\frac{CR_0 - CR}{CR_0} \right) \times 100 \quad (4)$$

In this case, CR₀ and CR denote the corrosion rates in the absence and presence of sacrificial anodes, respectively.

3. RESULTS AND DISCUSSION

3.1 Free corrosion by weight loss

Before cathodic protection was introduced, the rate of corrosion was determined by measuring the weight loss of carbon steel under different operational conditions. Figure 3 shows the corrosion rate of carbon steel as a function of salt concentration, which corresponds to different solution resistivities. This was determined using the weight loss method. The data shows that the corrosion rate of carbon steel increases with higher salt concentrations, reaching its highest point in a 0.1N NaCl solution. This is because the high dissolved salts causing an increase in the conductivity of the salt solution [5], the steel undergoes corrosion due to the presence of the Cl⁻ ion where the Cl⁻ ion will break the passive layer of carbon steel[22].

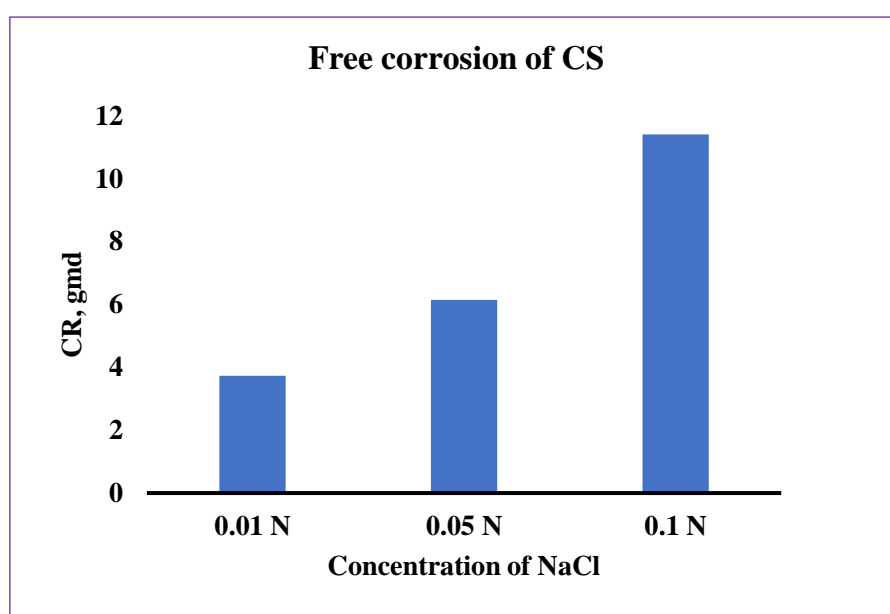


Fig. 3. Free corrosion of CS for different salt concentration

3.2 Cathodic Protection by ICCP

The protection potential for the carbon steel (CS) specimen was set at -0.85 V (SCE). Fig.4a shows the variation in potential of CS over time with and without cathodic protection. The data reveal that the protection potential of -0.85 V (SCE) decreases over time, indicating that the carbon steel is not fully protected and remains susceptible to corrosion. Fig.4 demonstrates that the free corrosion potential is significantly more positive than the protected specimen potential, highlighting the severe corrosion risk without protection, as illustrated in Fig.4. This underscores the necessity for cathodic protection in such environments. The specimen was examined before and after cathodic protection using the microscope, as shown in the Fig 4b and Fig4c, from the two figures, it is can observe that the surface of the specimen before protection appears darker than the surface after protection. This is due to the formation of a rust layer on the carbon steel surface.

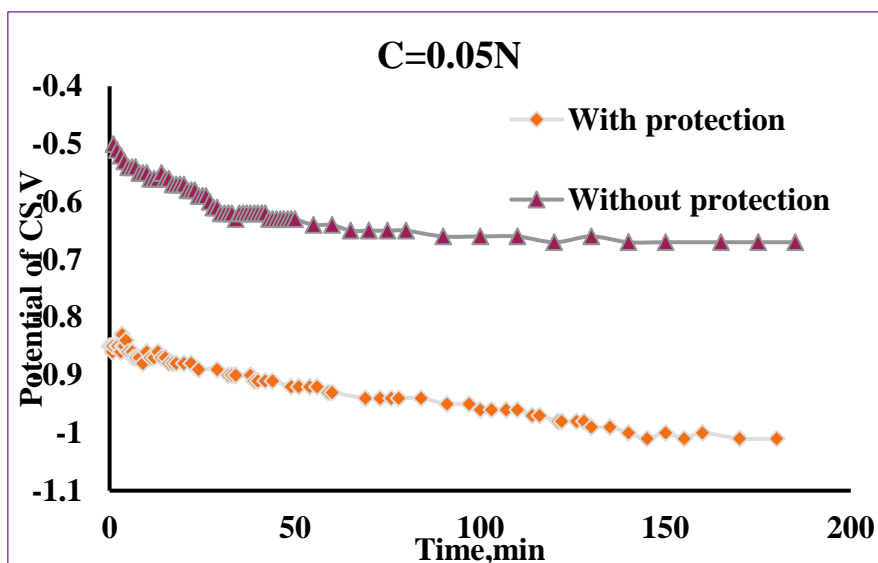


Fig. 4a. With and without cathodic protection curves of CS at 0.05N

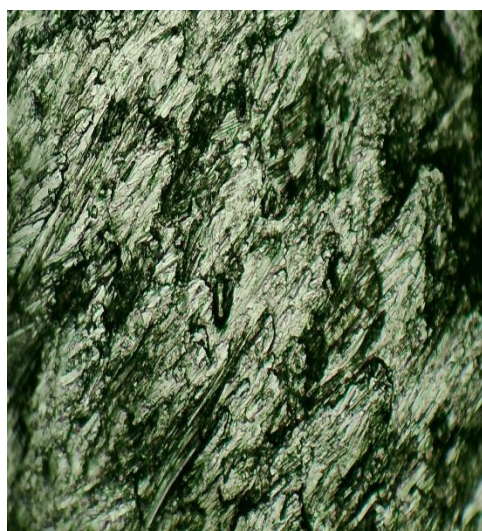


Fig. 4b. Microscope for carbon steel with production



Fig. 4c. Microscoup for carbon steel without protection

3.2.1 Effect of distance and area of anode

Figure 5a illustrates the corrosion rate of carbon steel (CS) under impressed current cathodic protection (ICCP) in a 0.05 N NaCl solution for various distances between the cathode (CS) and anode (graphite). The results show that a shorter distance results in a lower corrosion rate, with the optimal distance being 100 mm. Increasing the distance between the anode and the structure leads to a higher corrosion rate.

Figure 5b shows the relationship between the cathodic protection percentage (CP%) and the distance between the anode and cathode at 0.05 N NaCl. The CP% is highest at 100 mm, reaching 96%, indicating maximum efficiency when the anode and cathode are closest. At 200 mm, there is a noticeable decrease in CP% compared to 100 mm, and at 400 mm, the CP% drops further to 53%, demonstrating a decline in efficiency with increasing distance. The electrical resistance of increases with the distance between the anode and cathode. Greater resistance leads to less efficient current flow, which decreases the CP%. A shorter distance allows ions to move more efficiently between the electrodes, improving the reaction rates

and increasing the CP%. As the distance increases, ion transport becomes less efficient due to longer travel distances and potential diffusion limitations. this behavior had been observed by researchers[14,15,19]. Figures 6, to 10 show the potential of the carbon steel (CS) structure over time under various conditions Initially, the potential is approximately -500 mV vs. SCE without cathodic protection (CP). Following the application of impressed current cathodic protection (ICCP), the potential shifts negatively, reaching up to -1100 mV in some instances. The potential subsequently fluctuates, increasing and decreasing over time depending on the specific experimental conditions.

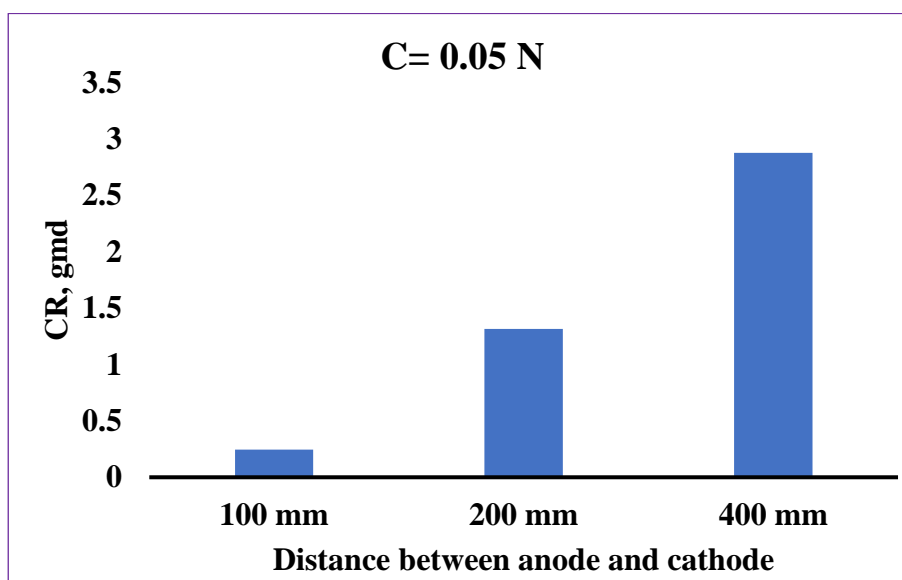


Fig. 5a. Effect of different distances on CR for CS at concentration= 0.05 N.

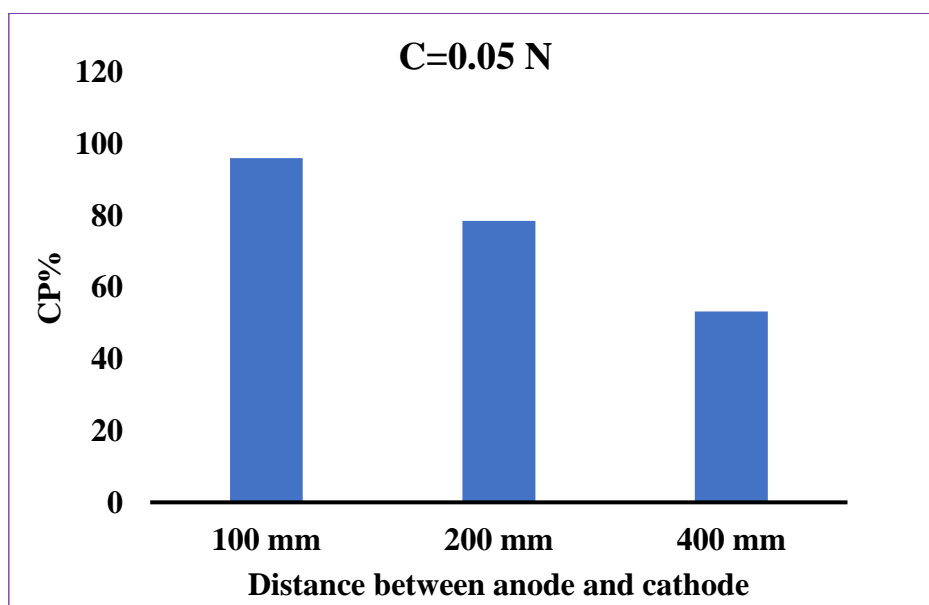


Fig. 5b. Effect of different distances on CP for CS at concentration=0.05 N.

Fig.6 shows the effect of distance between the cathode and anode on the potential of CS vs. time at area ratio (anode/ cathode) = 0.71. It indicates that when the distance is 100 mm, the potential is more positive than other distances. When the graphite is placed away from the carbon steel at 200 mm apart and 400 mm,

the CS potential becomes more negative leading to the increased probability of corrosion.

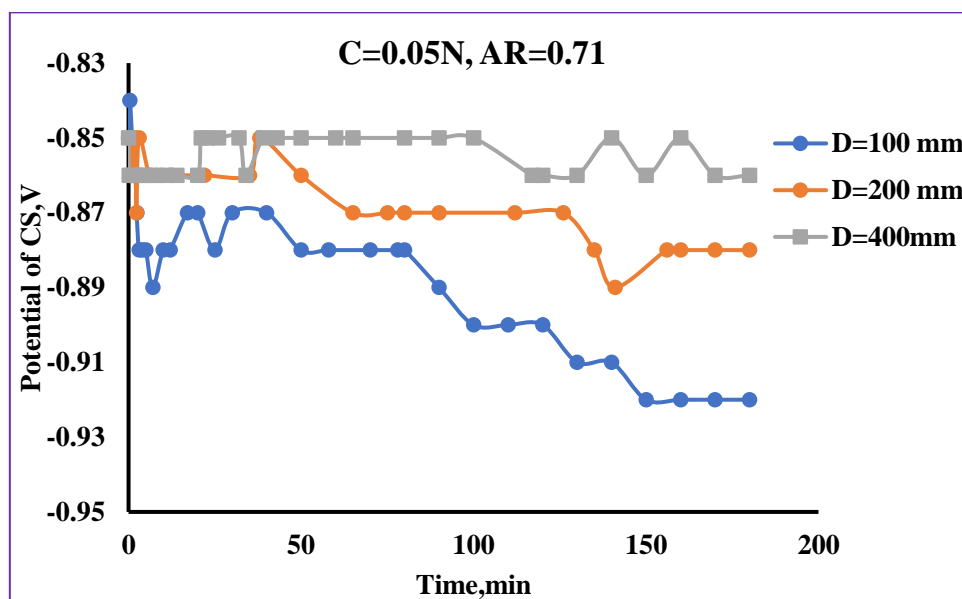


Fig. 6. Cathodic protection potential vs time for different anode to cathode distance (D).

Fig.7 demonstrates the relationship between the (CP%) and the distance between the anode and cathode for C= 0.1 N, with an anode to cathode (AR) of 0.71. It is evident that D=100 mm the CP% is highest (75%), and for D=200 mm, the CP% remains nearly the same, suggesting a minimal impact on efficiency, and d=400 mm the CP% drops to 56%, indicating reduced efficiency. Increasing the distance generally increases resistance to current flow. The higher salt concentration (0.1N) facilitates better ion transport, sustaining efficiency over shorter to intermediate distances. A smaller anode surface area compared to the cathode helps maintain electric field distribution, contributing to stable CP% at 200 mm and this agree with this research [24]

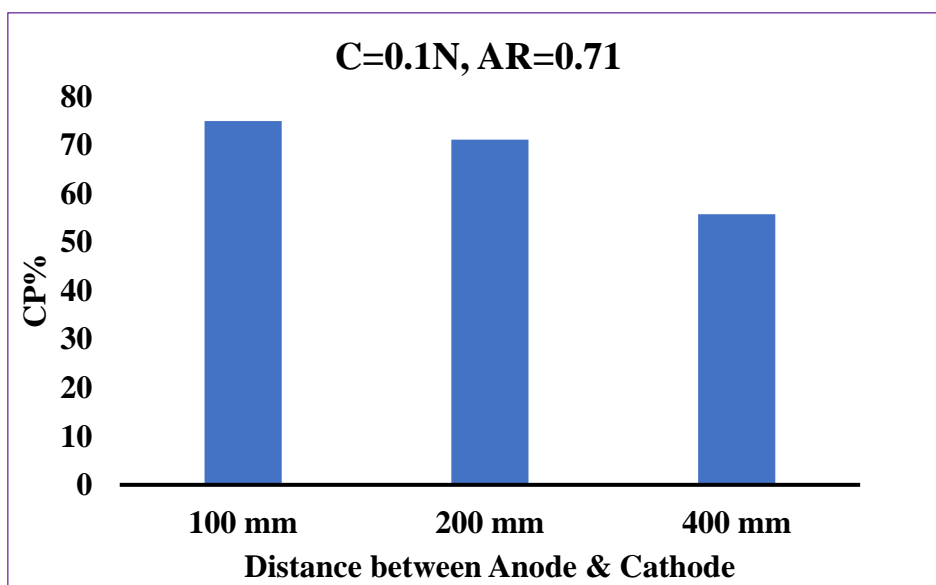


Fig. 7. Effect of different distances on CP for CS at concentration=0.1 N

Figure 8 shows the time history of the protection potentials for the different anode-to-cathode distances at $C=0.05N$, and $AR=1.29$. It can be seen that for 100 mm apart, the protection potential is the most negative indicating better protection as confirmed by Fig.5. With increasing distance between cathode and anode, the potential becomes more positive indicating the decrease in protection efficiency leading to an increase in the corrosion rate. Similar behavior has been observed in previous works[14,21]. Even with the increase in the ratio of the anode area to the cathode at 1.29 between, $D=100$ mm and $D=200$ mm, have close potentials. This convergence may be due to the increase in the reactive activity of the sites exposed to chlorine ion attack with increasing salt concentration and this is accepted with this research [17,22].

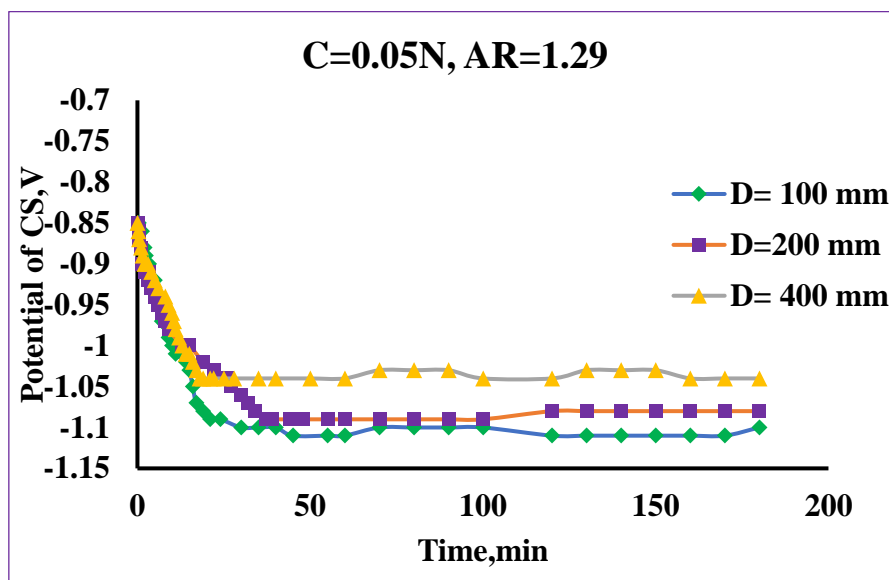


Fig. 8. Cathodic protection potential vs time for different anode to cathode distance (D).

This can be attributed to the surface area of the cathode that is subjected to the corrosion and hence affects the amount of electrons that will be released to protect the cathode and these results are in agreement with lotto and Popoola al[6].

In Figure 9, the relationship between the potential of cathode (CS) and time is clearly demonstrated. An increase in the distance at an area ratio of 0.71 leads to a decrease in the protection voltage below -0.95 V for 0.1 N salt concentrations. $D=100$ mm the shorter distance results in lower resistance in the electrochemical cell, leading to a quicker stabilization of the potential over time. The potential tends to be more negative initially and stabilizes faster, and at $D=400$ mm the longer distance increases the resistance, resulting in slower potential stabilization. The potential may be less negative initially and take longer to reach a stable state. Decreasing the distance between the anode and cathode typically leads to faster and more efficient potential stabilization in the electrochemical system.

It is furthermore, comparing Figs.9 with 10 indicates that the area ratio of the anode to cathode results in a noticeable increase in the protection potential. As the area ratio increases, the protection potential shifts to more negative indicating better cathodic protection. This can be attributed to the anode's ability to provide additional electrons as its area increases, leading to improved efficiency in cathodic protection. Similar behavior has been observed in previous works [14].

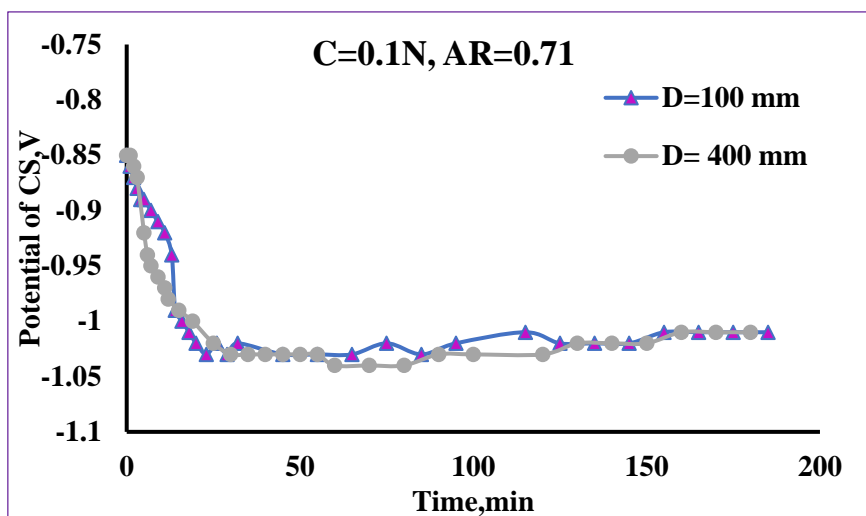


Fig. 9. Cathodic protection potential vs time for different anode to cathode distance (D).

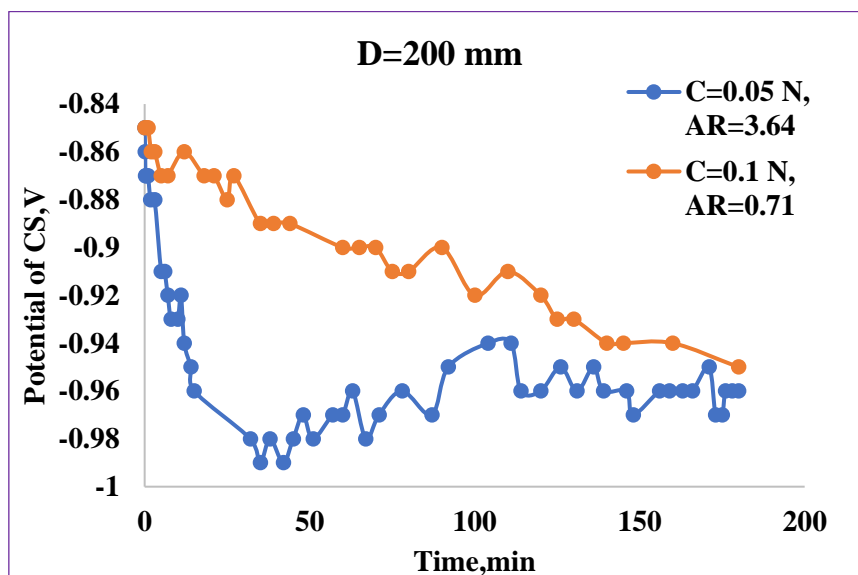


Fig. 10. Cathodic protection potential vs time at different concentrations and area ratio anode to cathode, distance (D=200 mm).

When the area ratio of cathode to anode increases to = and concentration at 0.05N, in cathodic protection by immersed current Fig.8 indicates the relation between carbon steel potential vs. time. The potential starts at -0.85 V and over time begins to drop to -0.99 V providing greater protection to the cathodic structure. After applying the protection current, the metal becomes shielded from corrosion. The decrease of the potential with time under cathodic protection is ascribed mainly to a decrease in oxygen reduction reaction on the cathode surface [27]. Fig.11 shows the relationship between the CP% and the distance between the anode and cathode at C=0.05 N, with varying anode-to-cathode area ratios (AR) it can be seen that increasing the distance generally increases resistance, which decreases CP%. This effect is more pronounced at lower area ratios. A larger AR (anode/ cathode) maintains the highest CP% for all distances due to better distribution of the electric field and more efficient ion transport [26]. Smaller anode areas can result in localized high current densities, which may lead to accelerated anode consumption and non-uniform protection of the cathode. Empirical evidence indicates that the efficacy of cathodic protection provided by an anode is significantly influenced by its surface area. Larger anodes can supply electrons more effectively, thereby enhancing cathodic protection and extending the interval between anode

replacements[6]. Therefore, the strategic design of anode area is essential for achieving optimal performance in impressed current cathodic protection (ICCP) systems and ensuring the long-term durability of the protected structure [25-27].

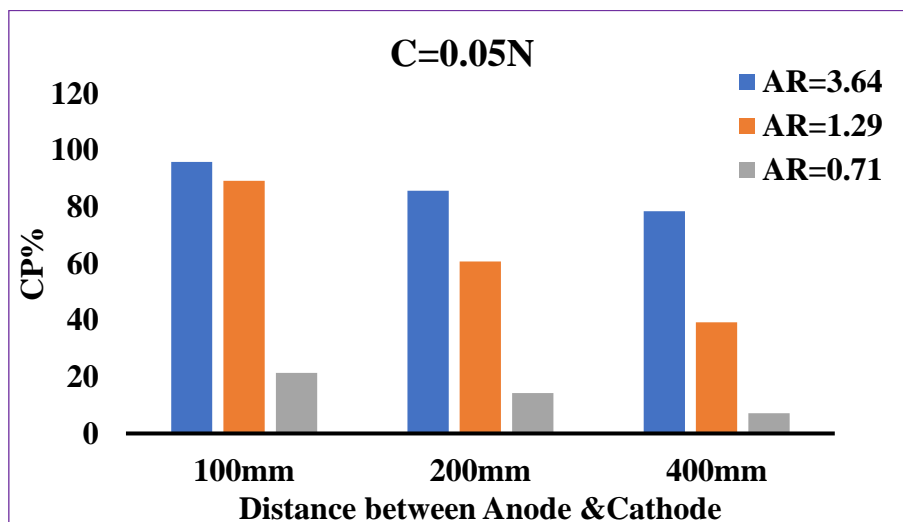


Fig. 11. Effect of different distances on CP for CS at concentration=0.05 N

3.2.2 Local cathodic protection by ICCP

Fig.12 and 13 show the trend of the protection potential with time, for the three specimens of CS connected at different locations from the connection point with the power source separated by distance “h”. Each figure considers different “h”. It can be seen that the CS1 (location A), representing the pipe section closest to the connection point with power source, is more negative than of CS2 (location B) which is more negative than CS3 (location C) [1,28]. In Fig.13, when the distance between the three locations is greater, the potential difference is more pronounced. The potential decay from the connection point to location of CS3, which is 1 meter away from the connection point, leads to enhanced local corrosion and a deficiency in local cathodic protection, similar behavior has been observed in previous works [5,6,29].

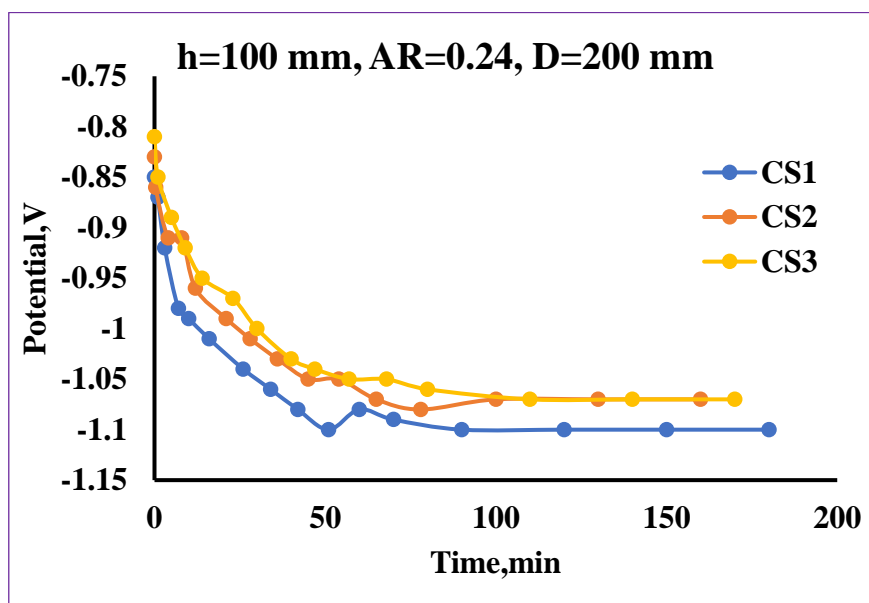


Fig.12. Protection Potential vs Time of the Three Local Positions, h= 100

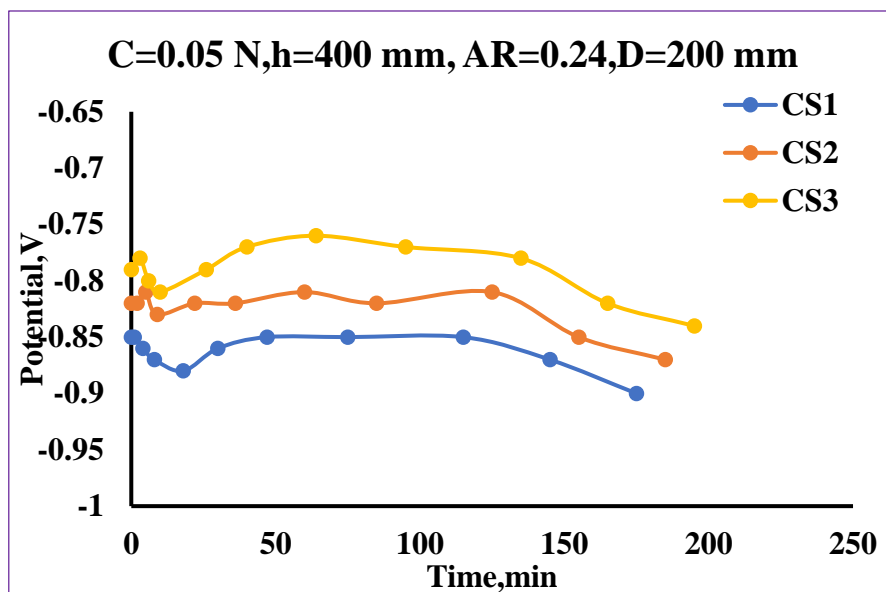


Fig.13. Protection Potential vs Time of the Three Local Positions, C=0.05 N, h= 400 mm.

In Fig.14, the cathodic protection is highest at the closest location (A) and decreases as you move away from the anode. It can be seen that when the position is 100 mm apart from the anode, the CP decreases by 3.5% from CS1 to CS2 and about 28.6% from CS2 to CS3. Additionally, the decrease in CP% between location A (CS1) and location B (CS2) is 35.6% for h=400 mm, and location B (CS2) to location C (CS3) is 17.8% for h=400 mm. The cathodic protection at position A has been higher than that at position B, whereas position B provides more protection than position C. This implies that the pipe portion located furthest from the power source connection point has a lower level of shielding. The main reason for this is the possibility of corrosion occurring on the surface of the steel pipe and this agrees with previous studies and this agrees with these papers [30,31].

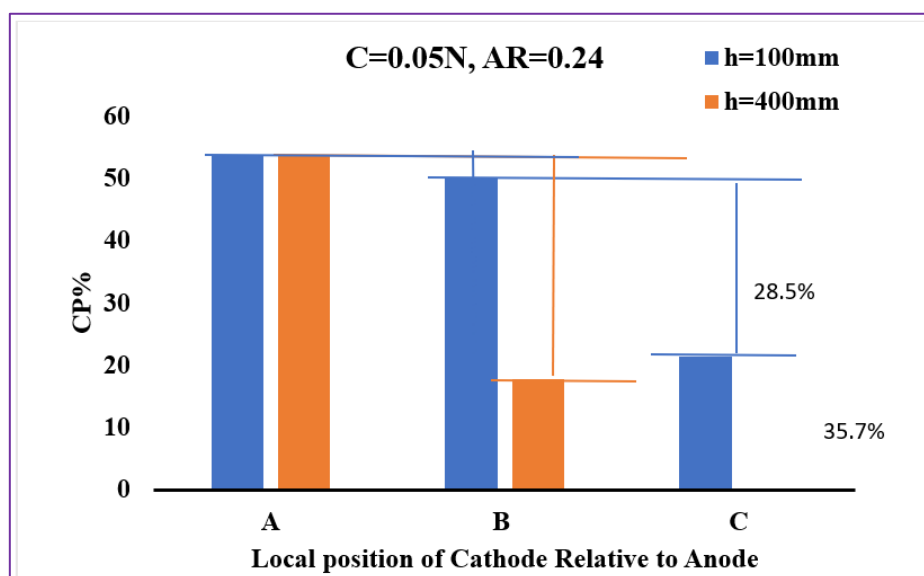


Fig. 14. CP% vs Time of the Three Local Positions from connection for AR= 0.24.

Fig.15 shows the potential of CS vs. time for three cathode specimens placed at a distance of 200 mm from the anode for $C=0.1$ N, and $h=100$ mm apart from each other, with area ratio of 0.24. There is an initial fluctuation in the curves for the first 40 minutes, followed by a slight stabilization after 65 minutes. Additionally, it is observed that the first carbon steel sample exhibits the most negative potential, followed by the second carbon steel sample, while the third sample is more positive than the previous ones. When the distance between the three specimens is increased to $h=400$ mm, as shown in Fig.16 under the same operating conditions, a gradual increase in the potentials of all three specimens is observed when moving away from the connection point with the power source due to potential decay. This indicates that the specimen protection decreases with the distance from the correction point with the power sources due to the potential decay leading to be exposed to corrosion. Additionally, there is a clear stabilization of the three potentials over time due to the complete transfer of electrolytic charges between the cathode and the solution.

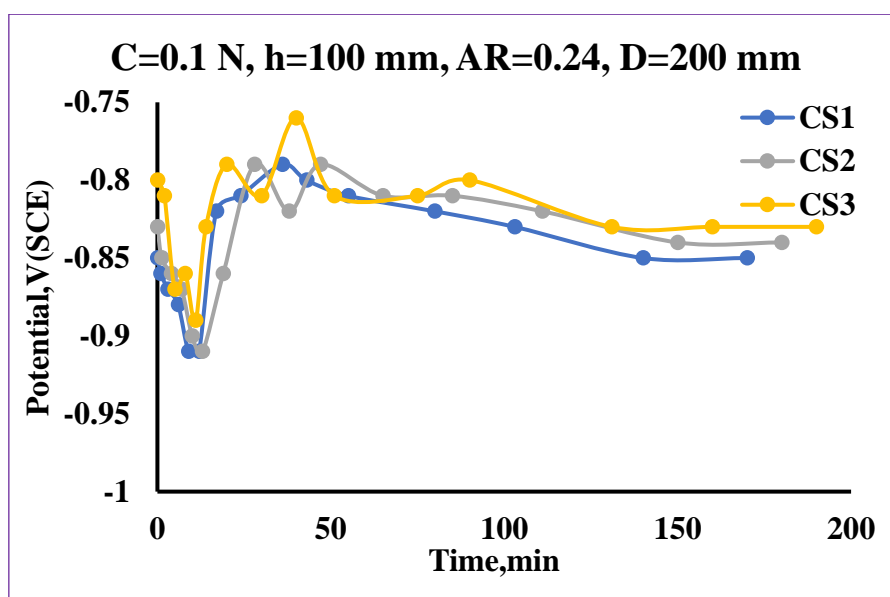


Fig.15. Protection Potential vs Time of the Three Local Positions, $C=0.1$ N, $h= 100$ mm.

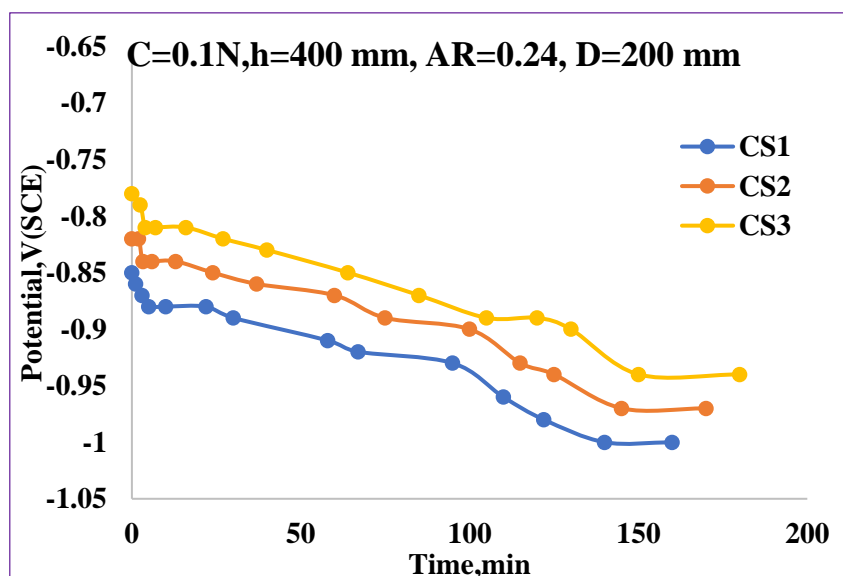


Fig.16. Protection Potential vs Time of the Three Local Positions, $C=0.1$ N, $h= 400$ mm.

Fig.17a Illustrates the values of cathodic protection percent for different specimen locations for different h values. It can be seen that the local cathodic protection percentage decreases when the specimen location moves away from the connection point with the power source. The closer the location to the power source connection point, the higher the cathodic protection percent for all interspaces (h). The histogram shows that the CP% for distance $h=100$ mm decreases by 1.9% when moving from A to B by 7.7% when moving from B to C. Additionally, the CP% at distance $h=400$ mm significantly decreases when the three specimens are spaced 40 mm apart from the initial distance. The cathodic protection percent decrease when moving from A to B is 9.6% and decreases by a similar percentage when moving from B to C, indicating consistent CP% among it. The specimen was examined at different local positions of cathodic protection using the microscope, as shown in Figures 17 b and 17c From the two figures, indicate that the specimen farther from the power source was more susceptible to corrosion compared to the sample closer to it.

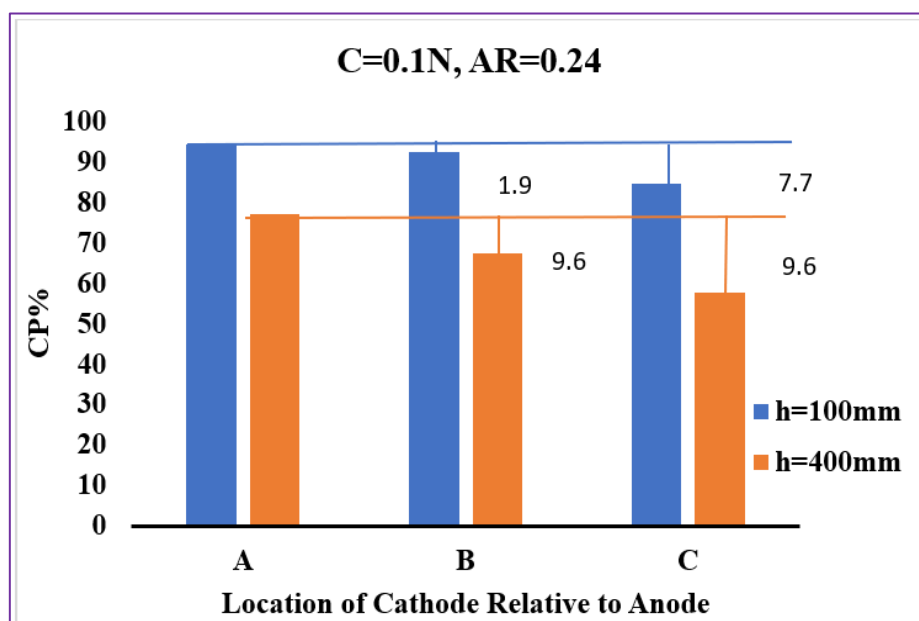


Fig. 17a. CP% vs Time of the Three Local Positions from connection for AR= 0.24.

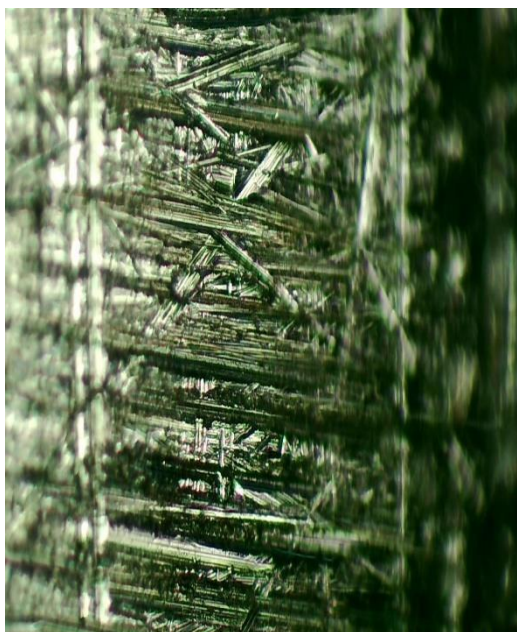


Fig. 17a. Microscoupe for CS1 at h=100 mm

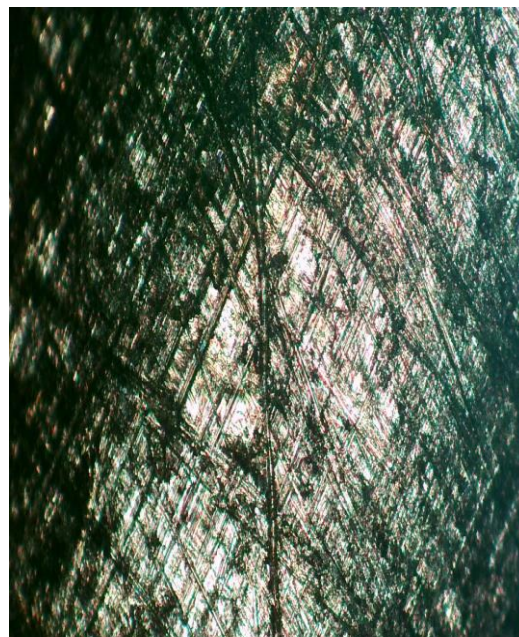


Fig 17b. Microscoupe for CS at h= 400 mm

Fig.18 demonstrates the projected trajectory of carbon steel over a period of time by increasing the surface area of the graphite anode to 0.43, while operating under conditions of $h = 100$ mm and $C = 0.05N$. After analyzing the curve, it is evident that there is a distinct fluctuation in the potentials of the three specimens, consistently moving towards increasingly negative values. A (CS1), located close the power source connection point, gets the most extensive protection. It is followed by component B (CS2), and eventually, C (CS3), which is exposed to the most significant corrosion due to its distance position from the power source. Illustrates the potential path of carbon steel over time when increasing the graphite anode area to 0.43 under operating conditions of $h = 100$ mm and $C = 0.05N$. Upon examining the curve, there is a clear fluctuation in the potentials of the three specimens, trending towards more negative values. A (CS1), being close to the connection point with the power source, receives the highest protection, followed by B (CS2), and finally, C (CS3), which experiences the highest corrosion due to its far location from the power source. This observation aligns with previous studies conducted by ([35,36]. In Fig.19 The following diagram shows the change in the potential of CS over time at a distance farther than the previous curved distance, with the new intesapce being $h=400$ mm from the cathodic location of the three electrodes. The first specimen (CS1) started with a protection potential of -0.86 mV, which is close to the protection standard potential for CS. The second specimen started with a slightly higher potential (more positive) but within the approximate protective range, initially at -0.83 mV. The third specimen had a much higher initial protection potential of -0.69 mV. Over time, within the protection system. It can be observed that the potentials become more negative with time and stabilize after approximately 75 min, indicating a steady state which agrees with previous observations [5,23, 34,35].

Figures 18 and 19 show that as the cathodic location moves farther away, the cathodic potential decreases.

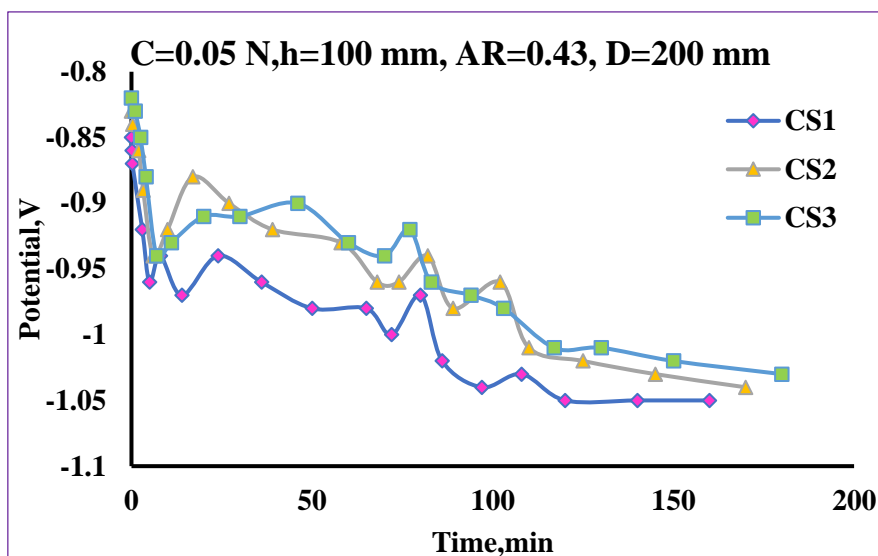


Fig. 18. Protection Potential vs Time of the Three Local Positions, C=0.05 N, h= 100 mm, AR=0.4, D= 200 mm.

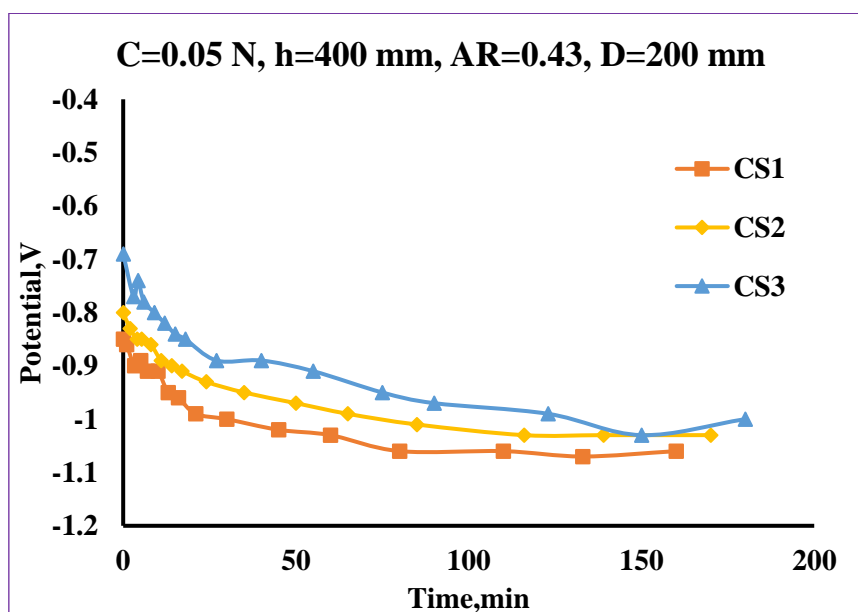


Fig. 19. Protection Potential vs Time of the Three Local Positions, C=0.05 N, h= 400 mm, AR=0.4, D= 200 mm.

Fig.20 shows the effect of two interspaces (h) for three specimens of CS at h=100 mm and h=400 mm for area ratio =0.43. The histogram illustrates the relationship between the effectiveness of CP% for three specimens at varying distances from the correction point with the power source. It shows that the highest protection level was achieved at a distance of 100 mm. Specifically, A(CS1) reached a protection level of 82% of CP%, B(CS2) achieved 78%, and C(CS3), the furthest from the power source, achieved 71%, the CP%. The decrease in CP% from location A to B is 3.6% form for h=100 mm and 6.8% for h=400 mm. The decrease in CP% from A to C is 10.7% from h=100 mm and the same for h=400 mm. This indicates that closer proximity to the connection point with the power source results in better cathodic protection, as has been reported by previous [23,36].

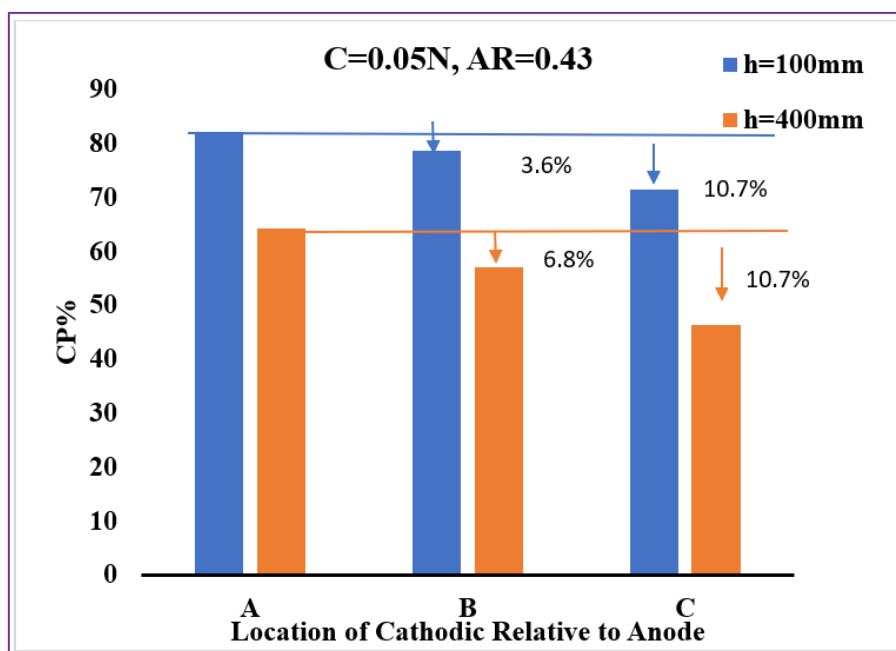


Fig. 20. CP% vs Time of the Three Local Positions from connection for AR= 0.43.

Fig.21 and 22 present the potential trend with time for AR=1.2 for the at different local cathodic protection h=100 mm and h=400 mm. It is clear that noticeable change in the protection potential at the specified values of local cathodic protection. The protection potential is low with an increase in the distance between three specimens. This is due to the ability of the anode to provide additional electrons while decreasing the distance from the connection point with the cathode. All above figures are started at a relatively different potential range within -950 to -850 mV relative to a distance increase between three specimens of cathodes [41].

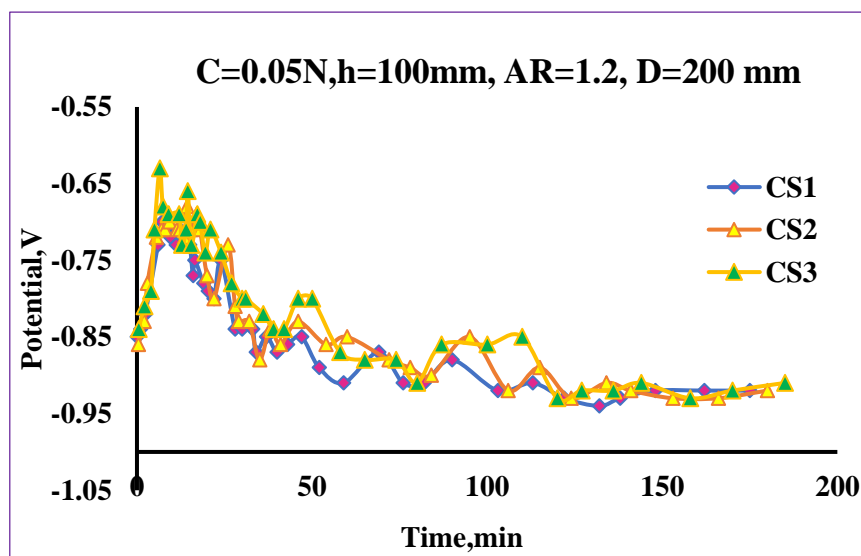


Fig. 21. Protection Potential vs Time of the Three Local Positions, C=0.05 N, h= 100 mm, AR=1.2, D= 200 mm.

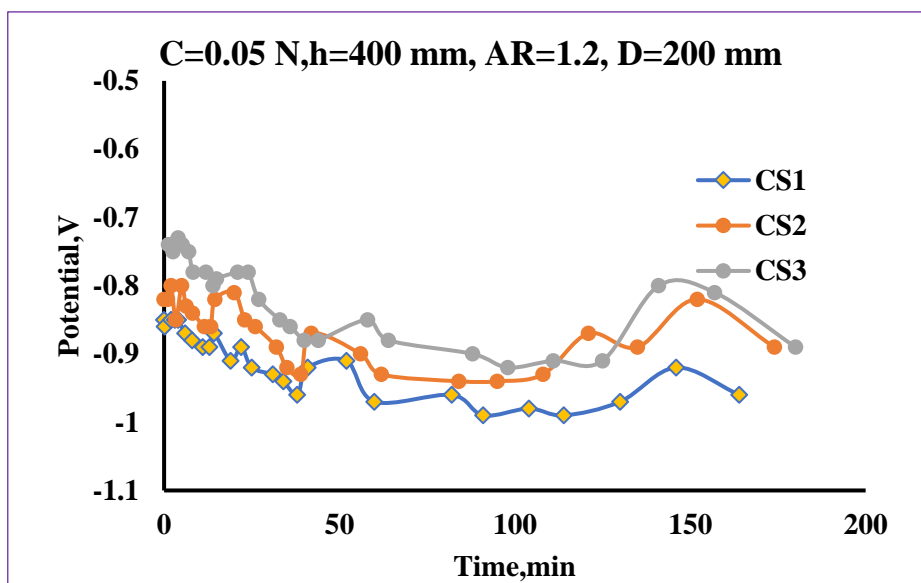


Fig. 22. Protection Potential vs Time of the Three Local Positions, C=0.05 N, h= 400 mm, AR=1.2, D= 200 mm.

Fig.23 depicts the cathodic protection percentage (CP%) for three carbon steel specimens at two different interspaces, h = 100 mm and h = 400 mm. At h = 100 mm, CP% is 3.6%, from A to B, and 39.3% from A to C, and CP% at h=400 mm is approximately 15.6% from A to B, 35.7% from A to C. The data suggests that cathodic protection efficiency decreases as the distance between the local position becomes far from the connection point with the power supply. This trend is consistent across all three samples of carbon steel, highlighting the importance of maintaining an optimal distance (100 mm in this case) for effective cathodic protection. It is crucial to consider these distances for industrial applications to ensure adequate protection of corrodible pipes and equipment that agrees with these works [23,38,39].

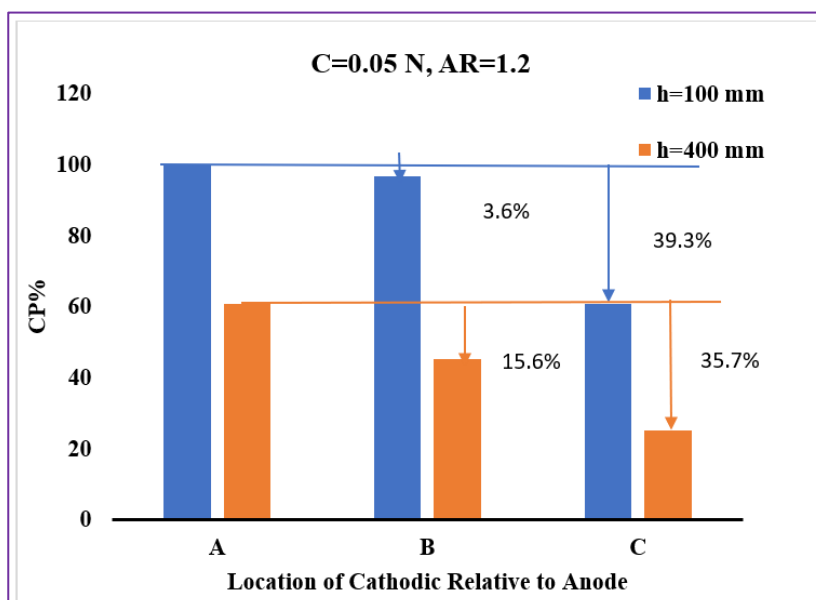


Fig. 23. CP% vs Time of the Three Local Positions from connection for AR= 1.2.

Fig.24 and 25 provide bar charts showing the cathodic protection percentage (CP%) versus the location for different distances (h) and concentrations. for 0.1N NaCl solution and 0.01N NaCl solution respectively for AR= 1.2.

Fig.24 shows that for 0.1N solution, the potential (V vs. SCE) for specimens CS1, CS2, and CS3 shows a strong protective effect across all locations with CP% of 96% for Dh=100 mm at location A and decreases to 86% at location C. As the distance h increases to 400 mm, the protective effect slightly decreases, suggesting that potential drop and time influence the effectiveness of cathodic protection leading to a decrease in CP% to become 88.5% at location A and 67% at location C. Fig.25 For lower concentrations of 0.01N, the protective effect is less, with CP% of 94% at A and 82% at C for h=100 mm. For h= 400 mm, the relevant values are 88% and 67%. This indicates that the potential (V vs. SCE) at lower concentrations does not sustain a high protection level over longer distances due to the potential decay, showing a sharper decrease in effectiveness over time [13,40]. The change in current with concentrations can be observed as shown in the Appendix table. A-2

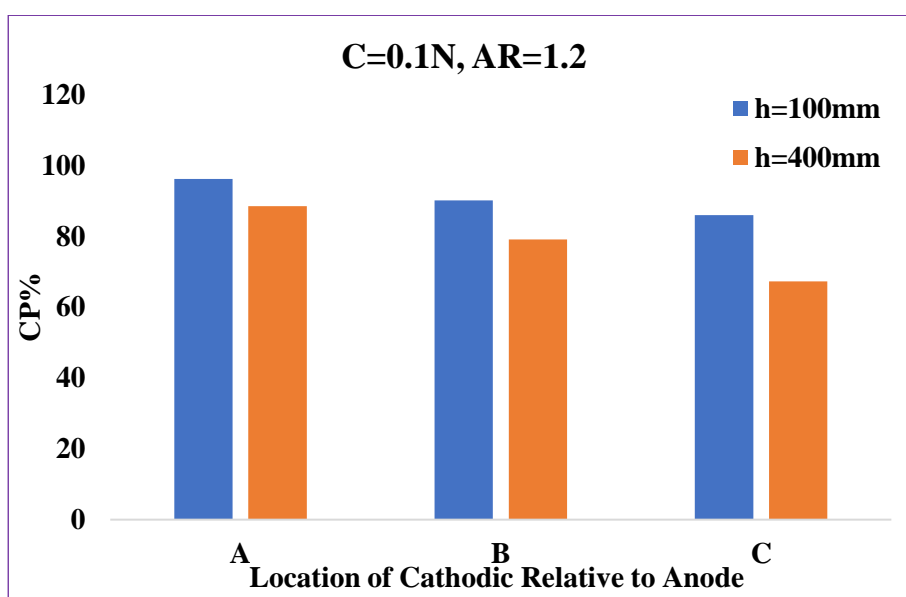


Fig. 24. CP% vs Time of the Three Local Positions from connection for C=0.1N NaCl, AR= 1.2.

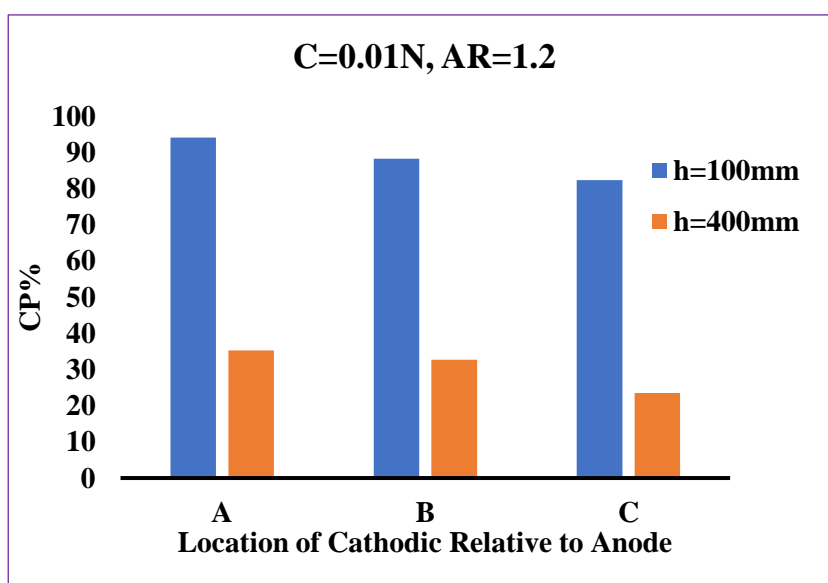


Fig. 25. CP% vs Time of the Three Local Positions from connection for 0.01N NaCl AR= 1.2.

4. CONCLUSION

This study shows that localized cathodic protection using impressed current cathodic protection (ICCP) significantly affects the surface of carbon steel pipes in industrial applications. At a constant temperature of 30°C, the protection efficiency was 100% for the section nearest to the power source, but decreased due to attenuation, reaching 87% in the middle section and 79% in the farthest section. The findings suggest that protection efficiency improves with an increase in the area ratio between the anode and cathode. However, increasing the area ratio among the three cathodic sections consistently reduces the overall protection efficiency under all operating conditions.

ACKNOWLEDGEMENTS

The authors are grateful to extend my thanks and gratitude to Al-Nahrain University and the Chemical Engineering Laboratories in the Chemical Engineering Department, which helped in providing the practical facilities and engineering equipment required for the research.

Author Contributions: The authors contributed to all parts of the current study.

Funding: This study received no external funding.

Conflicts of Interest: The authors declare no conflict of interest

NOMENCLATURE

CR	Corrosion rate(gmd)
CP	Cathodic protection
CS	Carbon steel

Appendix A

Table A. 1: Chemical composition if Carbon steel (EDX)

Element	Atomic %	Weight %
C	14.5	2
O	16.4	7.1
Si	1.2	0.8
Fe	68.0	90.1

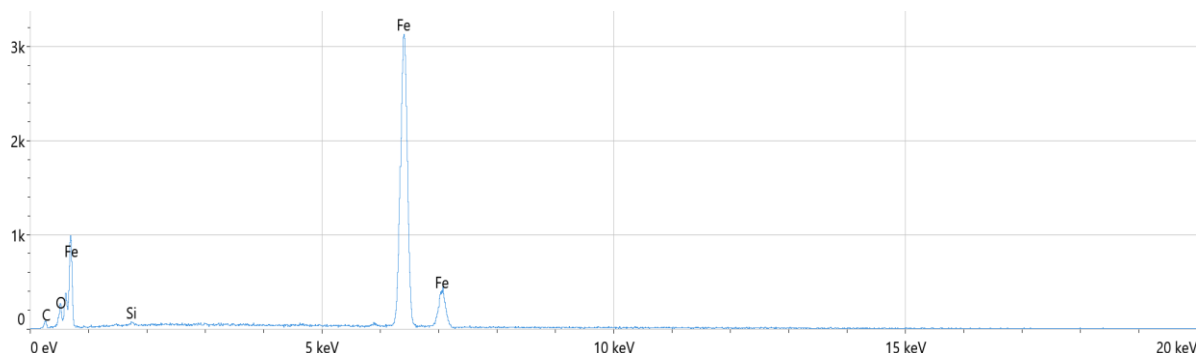


Fig.A.1: EDX Analysis of carbon steel specimen

Table A-2: Current protection at different concentration

Concentration	Current ,mA
0.01 N	1.5
0.05 N	6.5
0.1 N	9.4

References

[1] T. N. Guma, S. U. Mohammed, and A. J. Tanimu, “An experimental investigation of galvanic anode specifications for suitable cathodic corrosion protection of low carbon steel in Kaduna metropolitan soil,” *Am J Eng Res*, vol. 5, no. 2, pp. 109–119, 2016.

[2] P. Branko N, *CORROSION Principles and Solved Problems*. 2015.

[3] J. Hu, S. Wang, Y. Lu, and S. Li, “Case Studies in Construction Materials Investigation on efficiency of cathodic protection applied on steel in concrete cylinder with CFRP wrap serving as anode,” *Case Stud. Constr. Mater.*, vol. 17, no. June, p. e01389, 2022, doi: 10.1016/j.cscm.2022.e01389.

[4] ECCA, “The Basics of Corrosion Technical paper Contents Introduction,” 2011.

[5] Komalasari, Evelyn, I. D. R. Situmeang, and D. Heltina, “Cathodic protection on structures of carbon steel using sacrificial anode method for corrosion control,” *IOP Conf. Ser. Mater. Sci. Eng.*, vol. 845, no. 1, 2020, doi: 10.1088/1757-899X/845/1/012015.

[6] C. A. Loto and A. P. I. Popoola, “Effect of anode and size variations on the cathodic protection of mild steel in seawater and sulphuric acid,” 2011. Available online at <http://www.academicjournals.org/IJPS>, doi: 10.5897/IJPS11.537.

[7] C. Akintoye, R. Tolulope, and P. Abimbola, “Evaluation of cathodic protection of mild steel with magnesium anodes in 0 . 5 M HCL,” *Chem. Data Collect.*, vol. 22, p. 100246, 2019, doi: 10.1016/j.cdc.2019.100246.

[8] P. Refait, A. M. Grolleau, M. Jeannin, and R. Sabot, “Cathodic Protection of Complex Carbon Steel Structures in Seawater,” *Corros. Mater. Degrad.*, vol. 3, no. 3, pp. 439–453, 2022, doi: 10.3390/cmd3030026.

[9] R. B. Rebak, “Environmental Degradation of Engineered Barrier Materials in Nuclear Waste Repositories,” *Uhlig’s Corros. Handb. Third Ed.*, no. October, pp. 503–516, 2011, doi: 10.1002/9780470872864.ch36.

- [10] Z. Ahmad, *Principles of corrosion engineering and corrosion control*. Elsevier, 2006.
- [11] S. A. Ajeel and G. a Ali, "Variable Conditions Effect On Polarization Parameters Of Impressed Current Cathodic Protection Of Low Carbon Steel Pipes Received on : 7 / 3 / 2007 .," *Eng Tech*, vol. 26, no. 6, 2007.
- [12] E. Redaelli, F. Lollini, and L. Bertolini, "Cathodic protection with localised galvanic anodes in slender carbonated concrete elements," *Mater. Struct.*, vol. 47, pp. 1839–1855, 2014.
- [13] F. K. Matloub, M. M. Sulaiman, and Z. N. Shareef, "Investigating the effect of PH and salt concentration on cathodic protection of pipe-lines," *Int. J. Mech. Eng. Technol.*, vol. 9, no. 5, pp. 474–480, 2018.
- [14] S. Bhuiyan, D. Law, L. Ward, and J. Saliba, "The effects of anode distance and corrosion activity on current distribution for ICCP systems," vol. 03001, pp. 3–6, 2019.
- [15] E. S. Avianto *et al.*, "Pipeline Corrosion Protection Simulation of Cathodic Protection Method Againsts Electrochemical Potential Distribution," *IOP Conf. Ser. Earth Environ. Sci.*, vol. 519, no. 1, 2020, doi: 10.1088/1755-1315/519/1/012044.
- [16] M. A. BAWA, M. H. IBRAHIM, A. U. BABUJE, and E. E. AKABUIKE, "Investigation on the Potentials of Locally Produced Anodes for Impressed Current Cathodic Protection of Pipelines in Aggressive Environment," *IRE Journals*, vol. 3, no. 11, pp. 80–85, 2020.
- [17] P. Li and M. Du, "Effect of chloride ion content on pitting corrosion of dispersion-strengthened-high-strength steel," *Corros. Commun.*, vol. 7, pp. 23–34, 2022, doi: 10.1016/j.corcom.2022.03.005.
- [18] A. A. A. Beden, B. O. Hasan, and H. K. Sabti, "Cathodic protection of carbon steel using zinc and magnesium as sacrificial anodes in different conductivity solutions".
- [19] S. T. Abbas and B. O. Hasan, "Corrosion of carbon steel in formic acid as an organic pollutant under the influence of concentration cell," *J. Pet. Res. Stud.*, vol. 10, no. 2, pp. 76–94, 2020, doi: 10.52716/jprs.v10i2.352.
- [20] B. O. Hasan and M. F. Abdul-Jabbar, "CATHODIC PROTECTION OF CARBON STEEL IN 0.1N NaCl SOLUTION UNDER FLOW CONDITIONS USING ROTATING CYLINDER ELECTRODE," *J. Eng.*, vol. 18, no. 04, pp. 403–414, 2023, doi: 10.31026/j.eng.2012.04.02.
- [21] J. Kilbane, "Determining the Source of H₂S on an Offshore Oil Production Platform," no. March, 2017, doi: 10.1201/9781315157818-18.
- [22] S. Novita, E. Ginting, and W. Astuti, "Analisis Laju Korosi dan Kekerasan pada Stainless Steel 304 dan Baja Nikel Laterit dengan Variasi Kadar Ni (0, 3, dan 10%) dalam Medium Korosif," *J. Teor. dan Apl. Fis.*, vol. 6, no. 1, pp. 21–32, 2018.
- [23] L. Bouffier *et al.*, *Bipolar electrochemistry To cite this version : HAL Id : hal-03516326*. 2022.
- [24] B. Boz, T. Dev, A. Salvadori, and J. L. Schaefer, "Review—Electrolyte and Electrode Designs for Enhanced Ion Transport Properties to Enable High Performance Lithium Batteries," *J. Electrochem. Soc.*, vol. 168, no. 9, p. 090501, 2021, doi: 10.1149/1945-7111/ac1cc3.
- [25] W. Yodsudjai and S. Rakvanich, "Experimental study on anode life and effective distance of sacrificial cathodic protection in reinforced concrete," *Eng. J.*, vol. 24, no. 6, pp. 159–169, 2020, doi: 10.4186/ej.2020.24.6.159.
- [26] M. Bushman & Associates Inc., "Impressed Current Cathodic Protection System Design by," *Corros. Rev.*, vol. 24, no. 1–2, pp. 40–62, 2006.
- [27] O. I. Sekunowo, G. I. Lawal, S. I. Durowaye, and E. C. Igwebuikwe, "Effect Of Carbon Doped Aluminium On Corrosion Response Of Galvanised Steel In Seawater," *Int. J. Sci. Technol. Res.*, vol. 3, no. 8, pp. 57–63, 2014, [Online]. Available: www.ijstr.org
- [28] N. Hammouda, H. Chadli, G. Guillemot, and K. Belmokre, "The Corrosion Protection Behaviour of Zinc Rich Epoxy Paint in 3% NaCl Solution," *Adv. Chem. Eng. Sci.*, vol. 01, no. 02, pp. 51–60, 2011, doi: 10.4236/aces.2011.12009.
- [29] S. Uiyen, D. Law, L. Ward, and J. Saliba, "The effects of anode distance and corrosion activity on current distribution for ICCP systems," *MATEC Web of Conferences*, vol. 289. 2019. doi: 10.1051/mateconf/201928903001.
- [30] L. C. Matos and J. I. Martins, "Analysis of an educational cathodic protection system with a single

- drainage point: Modeling and experimental validation in aqueous medium,” *Materials (Basel)*., vol. 11, no. 11, pp. 1–10, 2018, doi: 10.3390/ma11112099.
- [31] A. H. Al-Moubaraki and I. B. Obot, “Corrosion challenges in petroleum refinery operations: Sources, mechanisms, mitigation, and future outlook,” *J. Saudi Chem. Soc.*, vol. 25, no. 12, 2021, doi: 10.1016/j.jscs.2021.101370.
- [32] O. M. Abdulwaheed, B. O. Hasan, and S. M. Alzurajji, “The effect of different heavy metals pollutants in refinery effluent on corrosion rate of carbon steel,” pp. 1–20.
- [33] H. M. Oghli, M. Akhbari, A. Kalaki, and M. Eskandarzade, “Design and analysis of the cathodic protection system of oil and gas pipelines, using distributed equivalent circuit model,” *J. Nat. Gas Sci. Eng.*, vol. 84, no. November, p. 103701, 2020, doi: 10.1016/j.jngse.2020.103701.
- [34] S. Edvlqj, R. Q. Wkh, I. Wkhru, F. Suhyhqwlrq, R. I. Slsholqh, and D. W. Jdv, “2Swlpl]Dwlrq Iru Wkh Fdwkrglf Surwhfwlrq V\Vwhp Edvhg Rq Qxphulfdo Vlpwodwlrq,” vol. 02038, 2020.
- [35] A. I. Marshakov and A. A. Rybkina, “Effect of Cathodic Protection Potential Fluctuations on the Corrosion of Low-Carbon Steels and Hydrogen Absorption by the Metal in Chloride Solutions with Nearly Neutral pH,” *Materials (Basel)*., vol. 15, no. 23, 2022, doi: 10.3390/ma15238279.
- [36] A. Mansouri, A. E. Binali, N. Khan, M. Zamanzadeh, and P. Taheri, “Three-dimensional modeling of in-ground cathodic protection systems with deforming anodes,” *Sci. Rep.*, vol. 11, no. 1, p. 1894, 2021.
- [37] Q. Zhang, L. Li, and B. Quan, “Research on Optimization of Cathodic Protection Effect of Buried Pipeline,” in *2020 International Conference on Computer Network, Electronic and Automation (ICCNEA)*, IEEE, 2020, pp. 347–351.
- [38] A. A. Atshan Å, B. O. Hasan Å, and M. Hali B, “Effect of Anode Type and Position on the Cathodic Protection of Carbon Steel in Sea Water,” *Res. Artic. Int. J. Curr. Eng. Technol. Accept.*, vol. 3, no. 5, 2017, [Online]. Available: <http://inpressco.com/category/ijcet>
- [39] Y. Zhou, X. Zheng, F. Xing, L. Sui, Y. Zheng, and X. Huang, “Investigation on the electrochemical and mechanical performance of CFRP and steel-fiber composite bar used for impressed current cathodic protection anode,” *Constr. Build. Mater.*, vol. 255, p. 119377, 2020.
- [40] F. Varela, M. Y. Tan, and M. Forsyth, “Electrochemical Method for Studying Localized Corrosion beneath Disbonded Coatings under Cathodic Protection,” *J. Electrochem. Soc.*, vol. 162, no. 10, pp. C515–C527, 2015, doi: 10.1149/2.0301510jes.
- [41] S. L. Lawal, S. A. Afolalu, T. C. Jen, and E. T. Akinlabi, “Corrosion Control and its Application in Marine Environment - A Review,” *Solid State Phenom.*, vol. 355, no. February, pp. 61–73, 2024, doi: 10.4028/p-634sdi.
- [42] J. A. Rogers, A. A. Maznev, M. J. Banet, and K. A. Nelson, *Optical generation and characterization of acoustic waves in thin films: Fundamentals and applications*, vol. 30. 2000. doi: 10.1146/annurev.matsci.30.1.117.
- [43] S. A. SADEK, “Corrosion of Carbon Steel in Acidic Salt Solutions Under Flow Conditions,” p. 116, 2012.